Depolarization activates the phosphoinositide phosphatase Ci-VSP, as detected in *Xenopus* oocytes coexpressing sensors of PIP_2

Yoshimichi Murata[1,2*] and Yasushi Okamura[1,2,3]

[1]*Section of Developmental Neurophysiology, Okazaki Institute for Integrative Bioscience,* [2]*National Institute for Physiological Sciences, National Institutes of Natural Sciences, and* [3]*Graduate University for Advanced Studies, Higashiyama 5-1, Myodaijicho, Okazaki, Aichi 444-8787, Japan*

Voltage-evoked signals play critical roles in neural activities, muscle contraction and exocytosis. *Ciona* voltage-sensor containing phosphatase (Ci-VSP) consists of the transmembrane voltage sensor domain (VSD) and a cytoplasmic domain of phosphoinositide phosphatase, homologous to phosphatase and tensin homologue deleted on chromosome 10 (PTEN). Previous experiments utilizing potassium channels as the sensor for phosphoinositides have demonstrated that phosphatase activities of Ci-VSP are voltage dependent. However, it still remained unclear whether enzyme activity is activated by depolarization or hyperpolarization. Further, a large gap in voltage dependency was found between the charge movement of the VSD and potassium channel-reporting phosphatase activities. In this study, voltage-dependent dynamics of phosphoinositides mediated by Ci-VSP were examined by confocal imaging and electrical measurements in *Xenopus* oocytes. Imaging of phosphatidylinositol-4,5-bisphosphate (PtdIns(4,5)P_2) using green fluorescent protein (GFP)-tagged pleckstrin homology (PH) domains from phospholipase C δ subunit (PLC-δ) showed that PtdIns(4,5)P_2 concentration is reduced during depolarization. In the presence of Ci-VSP, IRK1 channels with higher sensitivity to phosphoinositide than GIRK2 channels decreased their magnitude during depolarization over 0 mV, indicating that the PtdIns(4,5)P_2 level is reduced upon depolarization. KCNQ2/3 channels coexpressed with Ci-VSP exhibited voltage-dependent decay of the outward current that became sharper with higher depolarization in a voltage range up to 100 mV. These results indicate that Ci-VSP has an activity that depletes PtdIns(4,5)P_2 unlike PTEN and that depolarization-activated voltage sensor movement is translated into activation of phosphatase activity.

(Resubmitted 18 April 2007; accepted after revision 3 July 2007; first published online 5 July 2007)

Corresponding author Y. Okamura: Section of Developmental Neurophysiology, Okazaki Institute for Integrative Bioscience and National Institute for Physiological Sciences, National Institutes of Natural Sciences, Higashiyama 5-1, Myodaijicho, Okazaki, Aichi 444-8787, Japan. Email: yokamura@nips.ac.jp

[*] Present address: Department of Physiology I, Tohoku University Graduate School of Medicine, Sendai 980–8575, Japan

Changes in membrane potential play diverse biological roles, including electrical signalling in neurons, muscle and endocrine cells (Hille, 2001), phagocytosis in blood cells (Demaurex *et al.* 1993; DeCoursey *et al.* 2000), fertilization of eggs (Jaffe, 1976) and development of embryos (Levin *et al.* 2002). Voltage-gated ion channels are the key membrane proteins that mediate voltage-evoked cell signalling. Voltage-gated sodium, calcium and potassium channels and hyperpolarization-activated cation (I_h) channels share two common modular structures, the voltage sensor domain (VSD) and the pore domain (Hille, 2001). The VSD has long been studied as a structure unique to voltage-gated ion channels that plays a critical role in sensing transmembrane potential to regulate gating of the ion channel pore (Bezanilla, 2000; Hille, 2001; Tombola *et al.* 2006).

Recently we identified a VSD-containing protein, Ci-VSP, based on genome information from a species of urochordate, *Ciona intestinalis* (Murata *et al.* 2005). Ci-VSP has four transmembrane segments similar to the VSD of voltage-gated channels, but lacks a pore domain. Instead, Ci-VSP contains a cytoplasmic region that shows high similarity to phosphatase and tensin homologue deleted on chromosome 10 (PTEN). *In vitro* synthesized recombinant polypeptide of this cytoplasmic region of Ci-VSP exhibits robust phosphatase activity with phosphatidylinositol-3,4,5-trisphosphate

This paper has online supplemental material.

 DOI: 10.1113/jphysiol.2007.134775

(PtdIns(3,4,5)P_3) as substrate (Murata *et al.* 2005) like PTEN (Maehama & Dixon, 1998). The fourth transmembrane segment of the VSD of Ci-VSP includes the signature pattern similar to that of the VSD of voltage-gated ion channels and shows asymmetrical capacitative currents (Murata *et al.* 2005) similar to gating currents of voltage-gated channels, indicating that VSD is a self-contained functional unit consistent also with other studies (Lu *et al.* 2001; Long *et al.* 2005; Sasaki *et al.* 2006; Ramsey *et al.* 2006; Okamura, 2007).

The activity of phosphoinositide phosphatase of Ci-VSP changes in a voltage-dependent manner, as suggested by measurements of the activities of potassium channels that depend on the concentration of phosphoinositides (Murata *et al.* 2005). Ci-VSP is thus a unique protein that directly translates electrical information to chemical signal. Ci-VSP and its orthologue proteins possibly provide the molecular basis for several voltage-evoked biological phenomena that have not been ascribed to ion channels (Jaffe, 1976; Zhang & Zhou, 2002). However, the following basic questions regarding mechanisms of operation of Ci-VSP remain to be answered. First, it is not clear whether hyperpolarization or depolarization induces phosphatase activity of Ci-VSP, since PtdIns(4,5)P_2 is the intermediate substance in the entire cascade of phosphoinositide turnover. In particular, the idea that Ci-VSP dephosphorylates exclusively PtdIns(3,4,5)P_3 does not explain why PtdIns(3,4,5)P_3, a minor population of phosphoinositide, can produce such a significant change of PtdIns(4,5)P_2 level. Second, voltage-dependent change of phosphatase activity reported by GIRK2 (Kir3.2) channel activities was saturated at depolarization, around +20 mV, at which only about 10–15% of the total charge of the voltage sensor moves (Murata *et al.* 2005). This gap of voltage dependency between the charge movement and phosphatase activity could either be due to a limited dynamic range of sensitivity of Kir channels to phosphoinositides, or to the intrinsic coupling property of Ci-VSP. To address these questions, we performed imaging analysis using green fluorescent protein (GFP)-tagged pleckstrin homology (PH) domains, which are known to translocate to the cell surface dependent on the change of concentration of PtdIns(4,5)P_2 (Stauffer *et al.* 1998; Varnai & Balla, 1998; Zhang *et al.* 2004) and PtdIns(3,4,5)P_3 (Varnai *et al.* 1999). We also examined voltage-dependent phosphatase activity using activities of both the IRK1 channel and the KCNQ2/3 channel, which depend on PtdIns(4,5)P_2 for activation. The PtdIns(4,5)P_2 level was remarkably reduced compared to that of the normal resting level upon depolarization, and voltage-dependent change of PtdIns(3,4,5)P_3 and PtdIns(4,5)P_2 concentration as detected by the GFP-fused PH domain occurred in the same direction: both decreased upon depolarization. Further, potassium channels coexpressed with Ci-VSP exhibited graded activities up to 100 mV. These results indicate that Ci-VSP is a depolarization-activated phosphoinositide phosphatase in which dephosphorylation of PtdIns(4,5)P_2 is regulated by the VSD movement. This work has been partially reported in abstract form (Murata, 2006).

Methods

cDNAs and *in vitro* mutagenesis

cDNAs used in this study are identical to those described in our previous study (Murata *et al.* 2005) except for Ci-VSP mutants with mutation in the VSD and PH-domain proteins with GFP. KCNQ2/3 plasmids were provided by Dr D. McKinnon and Dr K. Nakajo. IRK1 plasmid was provided by Dr Y. Kubo. GIRK2 plasmid was provided by Dr M. Lazdunski. G-protein $\beta 1$ and $\gamma 1$ subunit plasmids were provided by Dr T. Nukada. The PH_{PLC}–GFP plasmid was a gift from Drs M. Takano, N. Uozumi and J. K. Lee (Zhang *et al.* 2004). The PH_{Btk}–GFP plasmid was a gift from Dr M. Fukuda (Fukuda *et al.* 1996). Ci-VSP mutants were constructed in pSD64 vector, which is a *Xenopus* oocyte expression vector. Mutation was introduced using the QuikChange kit (Stratagene). Primer sets used for mutagenesis were the forward sequence 5′-CCTTTTATAACGGGATGGC-3′, and the reverse sequence 5′-GCCATCCCGTTATAAAAGG-3′ for D151N, the forward sequence 5′-GTTATTTCATGCTGAATTTAGGATTAAGG-3′ and the reverse sequence 5′-CCTTAATCCTAAATTCAGCATGAAATAAC-3′ for D164N, the forward sequence 5′-CCTGGGAGGTTGCTAATGGTTTGATTATCG-3′ and the reverse sequence 5′-CGATAATCAAACCATTAGCAACCTCCCAGG-3′ for D186N, respectively (underlined nucleic acid indicates the mutated site). Mutation was confirmed by sequencing the primer overlapping the mutated site and the surrounding regions. cRNA was prepared from the linearized plasmid DNA by the mMessage mMachine Kit (Ambion).

Imaging of phosphoinositides using confocal microscopy in *Xenopus* oocyte

cRNAs of PH_{PLC}–GFP or PH_{Btk}–GFP were coinjected either with or without Ci-VSP in oocytes. Two to four days after injection, the oocytes were imaged using the FV300 confocal microscope system (Olympus) under two-electrode voltage clamp (TEVC) using AxoClamp2B (Molecular Devices). The bath solution was the same as for KCNQ2/3 recordings (see below). The oocytes were imaged using a 10× objective. For each episode, 80 images were collected for 2 s each (160 s) using Fluoview software (Olympus). Boxes were chosen as shown in Figs 1*A* and 2*A*, and fluorescence intensity in the areas of the boxes was calculated for each image and plotted

against time. Some oocytes showed non-specific change of cell morphology during recording, causing a drift of fluorescence intensity that occurred independently of membrane potential change. The results from these cells were excluded from analysis. All experiments were carried out at 22–24°C.

Two-electrode voltage clamp (TEVC) recordings in *Xenopus* oocytes

Before surgery, the frogs were anaesthetized by immersing in water containing 0.15% Tricaine. Isolated oocytes were treated with collagenase (1 mg ml^{-1}, S-1, Nitta Gelatin), and injected with approximately 50 nl of cRNA solution. All of the GIRK2 cRNAs were coinjected with Gβ1 and γ1. Experiments were performed according to the guidelines of the Animal Care Commitee of the National Institute for Physiological Sciences. The injected oocytes were incubated for 2–4 days at 18°C in ND96 solution (Goldin, 1992). Macroscopic current was recorded under two-electrode voltage clamp using a 'bath-clamp' amplifier (OC-725C-HV, Warner Co.). Stimulation, data acquisition and analysis were done on a Macintosh computer using an ITC-16 AD/DA converter and Pulse software (HEKA Electronik). Intracellular glass microelectrodes were filled with 3 M KCl (pH 7.2). The microelectrode resistance ranged from 0.1 to 0.6 MΩ. The bath solution contained 92 mM KCl, 3 mM $MgCl_2$, 4 mM KOH and 5 mM Hepes (pH 7.4) for Kir channels and 2 mM KCl, 92 mM NaCl, 3 mM $MgCl_2$, 4 mM NaOH and 5 mM Hepes (pH 7.4) for KCNQ2/3 channel recordings. Leak subtraction by the *P* over *N* protocol was not performed except for the measurements of 'gating' currents (Fig. 6*B*) and the data shown in Fig. 5*A*.

'Gating' current measurements

'Gating' current was measured in ND96 solution under TEVC. Holding potential was set to −60 mV for wild-type and D151N, and −80 mV for D164N/D186N. Leak currents and current derived from charging cell capacitance were cancelled using a *P*/–10 protocol in which a step pulse for subtraction was applied from a holding potential of −80 mV for wild-type and D151N, −90 mV for D164N/D186N. A holding potential was set deeper for D164N/D186N, because the *Q*–*V* curve is shifted leftward in this mutant and the risk of subtraction of the actual 'gating' current component with the *P*/–10 protocol needed to be minimized. Moved charge was calculated from OFF-current after components of cell capacitance were subtracted with the *P*/–10 protocol using Pulse + Plusefit software (HEKA Electronik). 'Gating' currents were verified by the following criteria: (1) moved charges are saturated at higher membrane potentials, and (2) the *Q*–*V* curve could be well fitted by a Boltzmann equation. Whereas ON-current is superimposed by the endogenous outward current at high depolarization such as over 100 mV, OFF-current upon hyperpolarization obtained under this condition gave a *Q*–*V* relationship indistinguishable from that obtained with the cut-open oocyte method over a wide range of test voltages, as previously reported (Murata *et al.* 2005). Results were indistinguishable from those recorded in the external solution utilized in the previous paper (Murata *et al.* 2005) that contained *N*-methyl-D-glucamine (NMDG)-methanesulphonate (data not shown).

Statistics

Error bars indicate S.D. Statistical significance was tested using the non-parametric Mann–Whitney test.

Results

Confocal imaging shows that the PtdIns(4,5)P_2 level is decreased upon depolarization and recovers upon hyperpolarization

The pleckstrin homology (PH) domain derived from PLC-δ is known to selectively bind to PtdIns(4,5)P_2 and translocate to the cell surface dependent on the concentration of PtdIns(4,5)P_2 (Stauffer *et al.* 1998; Varnai & Balla, 1998; Zhang *et al.* 2004). We examined the temporal change of PtdIns(4,5)P_2 by imaging PH-domain–GFP under confocal microscopy. *Xenopus* oocytes provide an ideal system for such analysis because of the opaqueness of the cytoplasm due to rich pigments and yolk and the translocation of the GFP-fused version of the PH-domain of PLC-δ (PH_{PLC}–GFP) can easily be quantified by measuring the intensity of fluorescence in the cell membrane (Zhang *et al.* 2004). A bright signal was detected on the cell contour in oocytes expressing PH_{PLC}–GFP. In oocytes only expressing PH_{PLC}–GFP, no significant change was seen either by depolarization or by hyperpolarization (Fig. 1*A* and *B* left panels). When Ci-VSP was coexpressed, the signals on the cell contour became gradually brighter on hyperpolarization (Fig. 1*B*, upper middle panel; online Supplemental material, movie 2). This change was reversed when the holding potential was set to 0 mV: the signal gradually faded (Fig. 1*B*, lower middle panel; $n = 7$; movie 1). Such change was not seen with a Ci-VSP mutant, R229Q/R232Q (Fig. 1*A* and *B*, right panels; $n = 4$; movie 3), which does not exhibit 'gating' current but is expressed on the cell surface of *Xenopus* oocytes (Murata *et al.* 2005).

It is known that PH_{PLC}–GFP binds to inositol 1,4,5-trisphosphate (Ins(1,4,5)P_3) and diffuses into the cytoplasm upon hydrolysis of PtdIns(4,5)P_2 by a phospholipase C (Varnai & Balla, 1998). When the cell membrane was depolarized in oocytes expressing Ci-VSP in ND96 solution, endogenous Ca^{2+}-activated Cl^- current, which is expected to be activated by

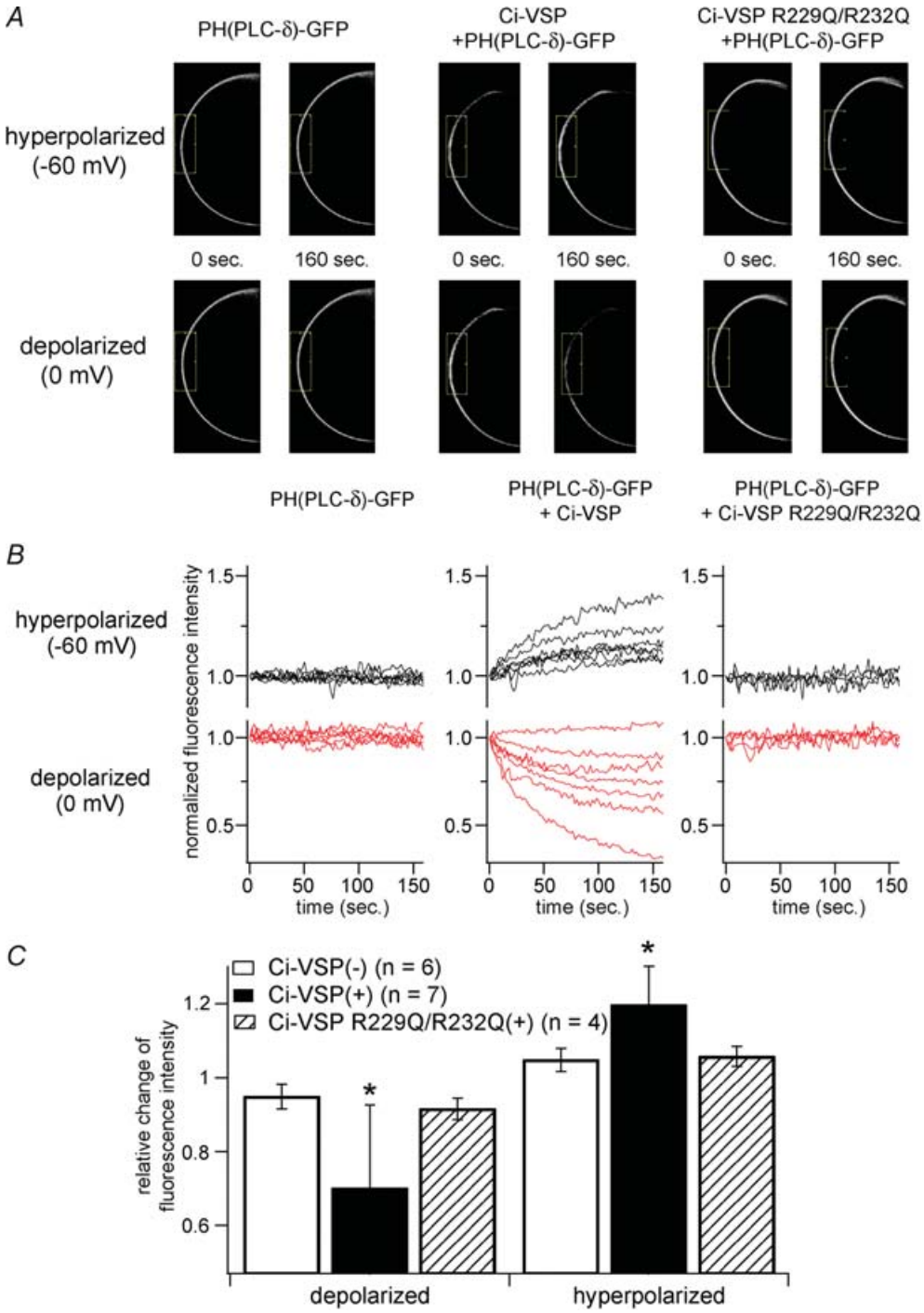

Figure 1. Confocal imaging with PtdIns(4,5)P_2 sensitive PH_{PLC}–GFP reports that PtdIns(4,5)P_2 is decreased by Ci-VSP during membrane depolarization

A, confocal images of oocytes under conditions of hyperpolarized (−60 mV) or depolarized (0 mV) membrane potential. GFP-fused PH domain of PLC-*δ* (PH_{PLC}–GFP) was coexpressed with (middle panels) or without (left panels) Ci-VSP in *Xenopus* oocytes. Images just before changing membrane potential (0 s) and at the last timing of the step (160 s) are indicated as pairs. PH_{PLC}–GFP coexpressed with Ci-VSP concentrated to and diffused from plasma membrane in the hyperpolarized (upper panel) and depolarized (lower panel) condition, respectively. When cell was inserted with two microelectrodes, it usually showed resting membrane potential ranging from −30 mV to −10 mV. Then the recording mode was switched to voltage clamp mode with holding potential of −60 mV for 160 seconds, stepped to 0 mV for 160 seconds, finally to −60 mV again for 160 seconds. Signals during the first hyperpolarizing stimulus are shown. Cells expressing PH_{PLC}–GFP with voltage-insensitive Ci-VSP mutant

$Ins(1,4,5)P_3$-induced calcium release, was not evoked (data not shown). This rules out the possibility that a decrease of PH_{PLC}–GFP upon depolarization was due to $Ins(1,4,5)P_3$ production by PLC endogenously expressed in *Xenopus* oocytes.

Imaging of the $PtdIns(3,4,5)P_3$-sensitive PH domain supports the hypothesis that dephosphorylation activity by Ci-VSP is turned on upon depolarization

We also performed imaging analysis of $PtdIns(3,4,5)P_3$ using the Btk-derived PH domain fused with GFP (PH_{Btk}–GFP), which is known to selectively detect $PtdIns(3,4,5)P_3$ (Salim *et al.* 1996; Varnai *et al.* 1999). Since a basal level of $PtdIns(3,4,5)P_3$ is usually extremely low at the resting condition, endogenous insulin receptors were stimulated to activate PI-3 kinase to increase $PtdIns(3,4,5)P_3$ by incubating oocytes with insulin ($8\,\mu$M) under voltage clamp to -60 mV (Fig. 2). As expected, the PH_{Btk}–GFP signal increased on the surface, reflecting the increase of $PtdIns(3,4,5)P_3$ production (Fig. 2*B*, upper three panels). Then, PH_{Btk}–GFP translocation was tested during depolarization and then during hyperpolarization. In most cases, clear depletion of PH_{Btk}–GFP from the cell surface occurs during depolarization, probably reflecting dephosphorylation of $PtdIns(3,4,5)P_3$ (Fig. 2*B*, in the middle column, middle panels with red traces). Such a decrease was not seen when prior activation of PI-3 kinase by insulin was not performed. In the hyperpolarizing episode following the depolarization, the signal of PH_{Btk}–GFP often increased. Decrease during depolarization or increase during the second episode of hyperpolarization was not seen in oocytes that spare Ci-VSP (Fig. 2*B*, left column) or express the voltage-insensitive form of Ci-VSP R229Q/R232Q (Fig. 2*B*, right column) with mutations in the VSD (Murata *et al.* 2005). We observed a minor decrease of fluorescence signal during depolarization from cells that express PH_{Btk}–GFP alone. However, these cells never showed an increase of GFP signal during hyperpolarization (Fig. 2*B*, left column, bottom panel with blue traces). Changes of intensity of Ci-VSP-expressing cells were significantly larger than those from cells expressing voltage-insensitive Ci-VSP or cells expressing just PH_{Btk}–GFP both in the protocols with depolarization and with hyperpolarization (Fig. 2*C*). These results indicate that Ci-VSP has phosphatase activity with $PtdIns(3,4,5)P_3$ as substrate, consistent with the *in vitro* measurements of the phosphatase activity using the glutathione-S-transferase-fused cytoplasmic region of Ci-VSP (Murata *et al.* 2005), and that $PtdIns(3,4,5)P_3$ concentration changes in the same direction as $PtdIns(3,4,5)P_3$ in response to changes in membrane voltage.

Evidence that phosphatase activity is activated upon depolarization (1): run-down of Kir activities

Imaging analysis confirmed that the $PtdIns(4,5)P_2$ concentration is reduced during depolarization and recovered during hyperpolarization, consistent with our previous observation of GIRK2 currents (Murata *et al.* 2005). From the high sequence similarity of Ci-VSP to PTEN, we originally predicted a scheme in which phosphatase activity is activated by hyperpolarization, and $PtdIns(3,4,5)P_3$ is dephosphorylated to $PtdIns(4,5)P_2$, since PTEN dephosphorylates $PtdIns(3,4,5)P_3$, but not $PtdIns(4,5)P_2$. However, given that $PtdIns(3,4,5)P_3$ is the minor species of phosphoinositide in the cell membrane and that its concentration is much lower than that of $PtdIns(4,5)P_2$, this scheme does not account for voltage-dependent change of Kir activities by membrane potential change, in particular, their marked reduction upon depolarization (Murata *et al.* 2005). Furthermore, the scheme also does not explain why both $PtdIns(3,4,5)P_3$ and $PtdIns(4,5)P_2$ changed their concentrations in the same direction in response to change of membrane potential (Figs 1 and 2). One alternative scheme could be that phosphatase activity is turned on during depolarization, rather than during hyperpolarization, and that the $PtdIns(4,5)P_2$ level is reduced by the phosphatase activity.

To test if reduction of $PtdIns(4,5)P_2$ occurs in a voltage-dependent manner, the run-down kinetics of Kir activity was examined at distinct levels of interval voltages ranging from 0 mV to 40 mV by measuring the Kir amplitude of GIRK2 channels every 500 ms (Fig. 3). As interval potentials were made more positive, Kir activities decreased more rapidly (Fig. 3*B* and *C*) consistent with the idea that depletion of $PtdIns(4,5)P_2$ occurs by voltage-regulated phosphatase activity.

If Ci-VSP depletes $PtdIns(4,5)P_2$ upon depolarization, the level of $PtdIns(4,5)P_2$ should be less than the normal resting level. To gain information about the extent to which the $PtdIns(4,5)P_2$ level is reduced upon

(R229Q/R232Q) did not exhibit such translocation (right panel). *B*, temporal change of fluorescence intensity of GFP under voltage clamp. The intensity was standardized by the initial intensity. Individual traces were obtained from different cells. In the cells shown in *A*, intensities in the boxed regions were measured. *C*, averaged change of fluorescence intensity from multiple cells. Minimal (depolarized) or maximal (hyperpolarized) intensity during each recording was corrected by the intensity at time zero in individual cell. Asterisks indicate a statistically significant difference ($P < 0.05$) from Ci-VSP(–) cells.

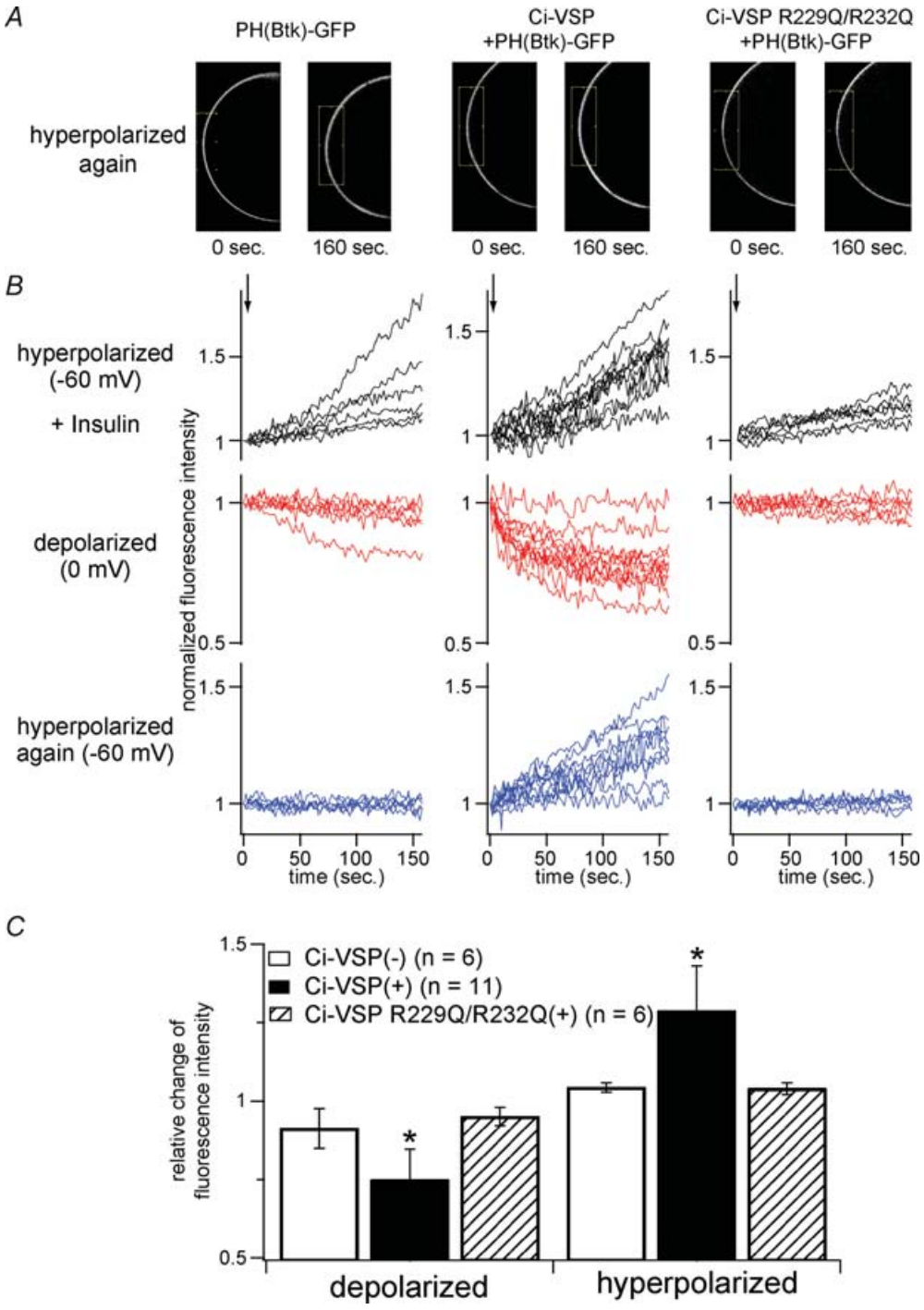

Figure 2. Btk-derived (PtdIns(3,4,5)P_3-sensitive) PH-domain fused with GFP reports that Ci-VSP decreases PtdIns(3,4,5)P_3 upon membrane depolarization

A, confocal images taken just before applying the second hyperpolarizing episode and just before the end of the episode in each example of the cell only with GFP-fused PH domain of Btk (PH_{Btk}–GFP) (left panels), with Ci-VSP and PH_{Btk}–GFP (middle panels) and with VSD mutant of Ci-VSP with PH_{Btk}–GFP (right panels). Oocytes were primed to activate PI-3 kinase to increase PtdIns(3,4,5)P_3 level by applying insulin (8 μM: applied in the time indicated by arrow in top panels of *B*). After insulin application, translocation of PH_{Btk}–GFP exhibited similar voltage dependence to that of PH_{PLC}–GFP: depolarization decreased the signal, whereas hyperpolarization increased the signal. *B*, temporal changes of fluorescence intensity during hyperpolarization (−60 mV) or depolarization (0 mV) are shown. Individual traces were obtained from different cells. Measured areas are indicated as boxes in *A*. *C*, statistical representation of *B*. Analysis was performed in a similar manner as in Fig. 1*C*. Asterisks indicate a statistically significant difference ($P < 0.05$) from Ci-VSP(–) cells.

depolarization compared with the normal level, we utilized the IRK1 (Kir2.1) channel, which has a higher affinity for PtdIns(4,5)P_2 than the GIRK2 channel and potentially serves as a sensitive indicator of PtdIns(4,5)P_2 less than 1 μM (Huang *et al.* 1998). When IRK1 was coexpressed with Ci-VSP and membrane potential was varied up to 60 mV, IRK1 activity gradually decreased as the membrane potential increased (Fig. 4*A*). In most cases, Kir current could be recovered from its depletion to the original current amplitude when the holding potential was reset to −60 mV ($n = 4$). Depolarization-induced run-down of Kir occurred in a time scale of 10 s (Fig. 4*C*, left) whereas recoveries of Kir currents by hyperpolarization to −60 mV took longer (Fig. 4*C*, right panels). Such depolarization-dependent decrease of Kir current was never observed (Fig. 4*B*, triangles) when IRK1 was coexpressed with an enzyme-defective form, C363S (Murata *et al.* 2005). Given that the affinity of IRK1 for PtdIns(4,5)P_2 is about 0.5 μM (Huang *et al.* 1998), PtdIns(4,5)P_2 is reduced to a level much lower than in the normal cell membrane. The significant rightward shift of voltage dependency of IRK1 current (red line) from that of GIRK2 (blue dotted line in Fig. 4*B*) is also consistent with the notion that the PtdIns(4,5)P_2 level is reduced by Ci-VSP activities upon depolarization.

Evidence that phosphatase activity of Ci-VSP is activated upon depolarization (2): decay of KCNQ2/3 channel is induced by depolarization

KCNQ2/3 potassium channels are known to underlie the M-current of neurons (Wang *et al.* 1998). Activities of KCNQ2/3 potassium channels are known to be sensitive to PtdIns(4,5)P_2 and their sensitivity to PtdIns(4,5)P_2 is one of the mechanisms that underlie inhibitory modulation by the muscarinic acetylcholine receptor (Zhang *et al.* 2003). In our previous report, KCNQ2/3 channels on coexpression with Ci-VSP exhibited voltage-dependent changes of their current magnitude, indicating that KCNQ2/3 also serves as a faithful reporter of phosphoinositides. Modulation of their activities by coexpressed Ci-VSP was examined in more detail. When KCNQ2/3 channels were expressed alone, delayed-rectifying potassium currents did not exhibit any decay (Fig. 5*A* upper panel). When Ci-VSP was coexpressed, the current amplitude saturates at the large depolarization and even decreases at higher voltage (Fig. 5*A* lower panel), resulting in a bell shaped *I–V* curve (Fig. 5*B*). Current traces show a slight decay during the depolarizing pulse. We suspect that such saturation of amplitude at higher voltage could be due to depletion of

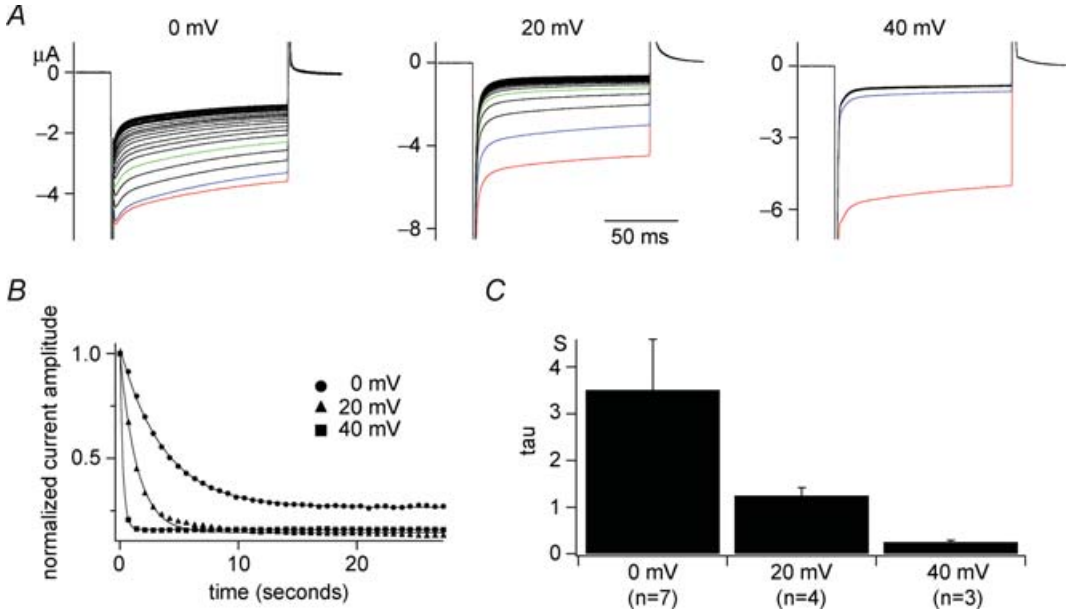

Figure 3. Voltage-dependent kinetics of run-down of GIRK2 current
A, families of Kir currents of GIRK2 channels when interval voltage was set to 0, 20 or 40 mV. Preceding these recordings, cells were held at −60 mV for 60 s. Raw current traces elicited during repetitive test pulses to −100 mV every 500 ms are superimposed. Following test pulses, cells were held to indicated potential levels for 250 ms. Red traces are for the first episodes, blue for the second and greens for the fifth episodes, respectively. Such voltage-dependent run-down does not occur when only the GIRK2 channel was expressed or coexpressed with the enzyme-defective Ci-VSP (C363S) (data not shown). *B*, plots of temporal changes of maximum Kir amplitudes from sets of data indicated in *A*. The curves were fitted with a single exponential. *C*, the averages of time constants for fitting the plots as in *B* from different cells. Time constants at 0 mV, 20 mV and 40 mV, were 3.51 ± 1.08 s ($n = 7$), 1.25 ± 0.17 s ($n = 4$), and 0.25 ± 0.04 s ($n = 3$), respectively.

PtdIns(4,5)P_2 by enhanced phosphatase activity of Ci-VSP upon depolarization.

With a long depolarizing pulse (2 s) to various levels of membrane potential, KCNQ2/3 current showed a decay pattern that becomes sharper as the membrane potential increases (Fig. 5*C*). The current decay could be fitted by single exponentials (data not shown). The time constants plotted against the membrane potential showed clear voltage dependency over a span of +100 mV (Fig. 5*D*). Oocytes expressing KCNQ2/3 with the enzyme-defective Ci-VSP (C363S) mutant (Murata *et al.* 2005) did not exhibit such decay (Fig. 5*C*, lower panel). Time constants of decay of KCNQ2/3 currents at 20 mV and 40 mV were significantly longer than those of decline of GIRK2 activities measured with interval potentials to the same levels (Fig. 3), possibly reflecting that GIRK2 channels require a higher concentration of PtdIns(4,5)P_2 for their channel activities than KCNQ2/3 channels.

Is voltage dependence of phosphatase activity in Ci-VSP derived from VSD?

In our previous report, when the two positive arginines in the S4 segment of Ci-VSP were replaced by glutamine

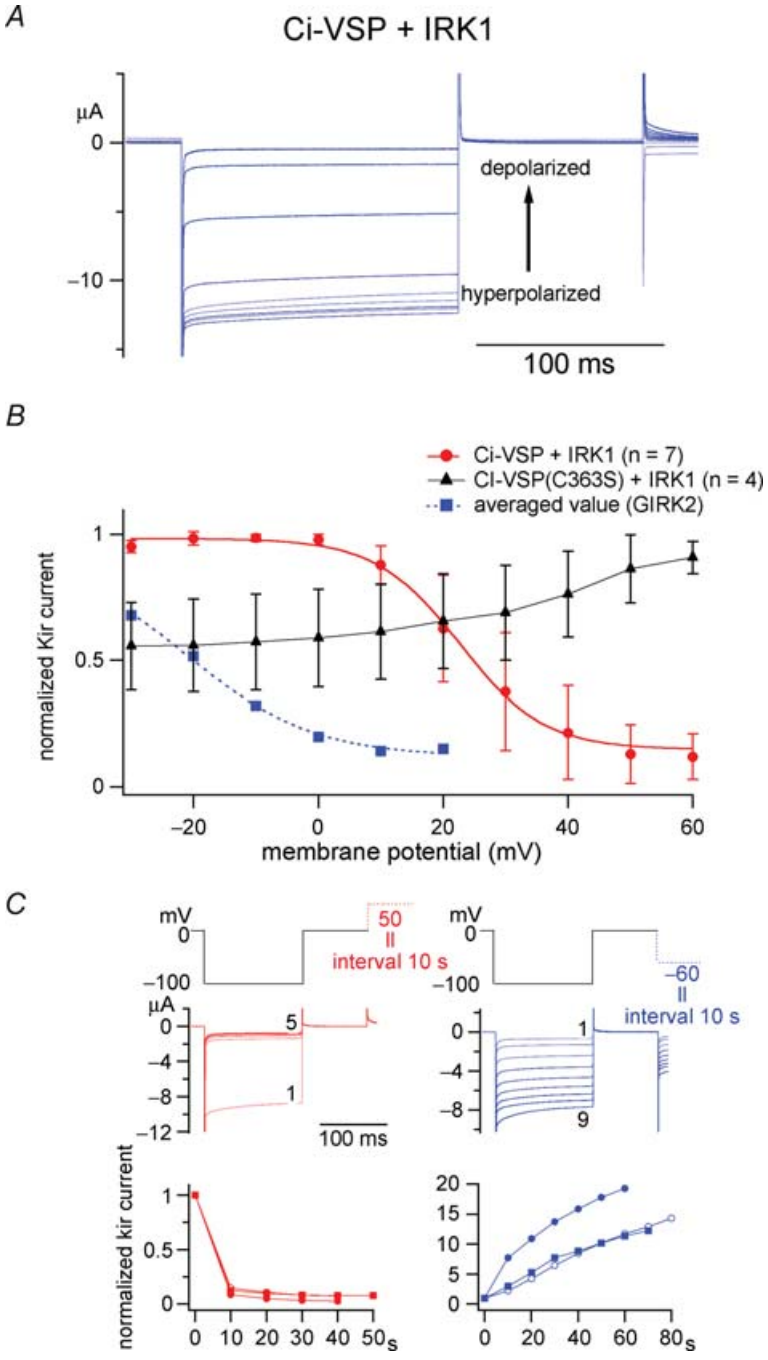

Figure 4. Changes in IRK1 (Kir2.1) channel activity report the enzymatic activity of Ci-VSP from 10 mV to 60 mV
A, representative traces of the current of PtdIns(4,5)P_2-sensitive IRK1 potassium channel coexpressed with Ci-VSP. Intervals were held to membrane potentials ranging from −30 mV to 60 mV. *B*, the dependence of relative amplitude of IRK1-derived currents on the interval voltages. IRK1 channel showed voltage-dependent decrease of the current from 10 to 60 mV (red), in a range more positive than that with GIRK2 (blue). IRK1 channels coexpressed with enzyme-defective Ci-VSP mutant (C363S) did not exhibit such changes in activity (black). Data of GIRK2 (dotted blue line) were adopted from our previous study (Murata *et al.* 2005). *C*, time-dependent change of Kir activities with depolarizing intervals to +50 mV (red) or with hyperpolarizing intervals to −60 mV (blue). The top panel indicates pulse protocols. In the middle panel, current traces evoked during repetitive test pulses to −100 mV are superimposed. Episode numbers are indicated for traces at the initial and last episode. Bottom panels show time-dependent plot of the Kir current. Values from four individual cells are shown by distinct symbols in both red and blue plots. The Kir amplitudes were standardized by those at zero time.

residues, it neither showed 'gating' current, nor voltage dependency of phosphatase activity as reported by potassium channel activities (Murata *et al.* 2005). This suggested that the voltage dependence of the phosphatase activity of Ci-VSP is derived from the nature of VSD. However, we could not rule out the possibility that this mutant of Ci-VSP did not adopt the normal conformation or proper folding in the cell membrane.

A critical test for whether voltage dependency of phosphatase activity is really derived from the VSD is to test how voltage dependency of phosphatase activity is altered when the properties of VSD are modified. For another experiment, we had constructed numerous VSD mutants of Ci-VSP. In this survey, one construct, D164N/D186N mutant with two mutations in the VSD (scheme in Fig. 6*A*), exhibited significantly slower kinetics than that of wild-type (Fig. 6*B*) and shifted the charge–voltage (Q–V) curve as compared with the wild-type (blue filled squares, Fig. 6*C*). Another mutant D151N (Fig. 6*A*), in which one negative charge in the S2 segment was neutralized by asparagine, exhibits faster kinetics of OFF-'gating' currents than the wild-type (Fig. 6*B*). The Q–V curve of OFF-'gating' currents (Q_{off}–V curve) showed a rightward shift as compared with that of the wild-type (red closed circle, Fig. 6*C*). In our recording conditions of TEVC, some endogenous outward current was activated by depolarization over 100 mV (traces in Fig. 6*B*). Nevertheless, such endogenous conductance gave only

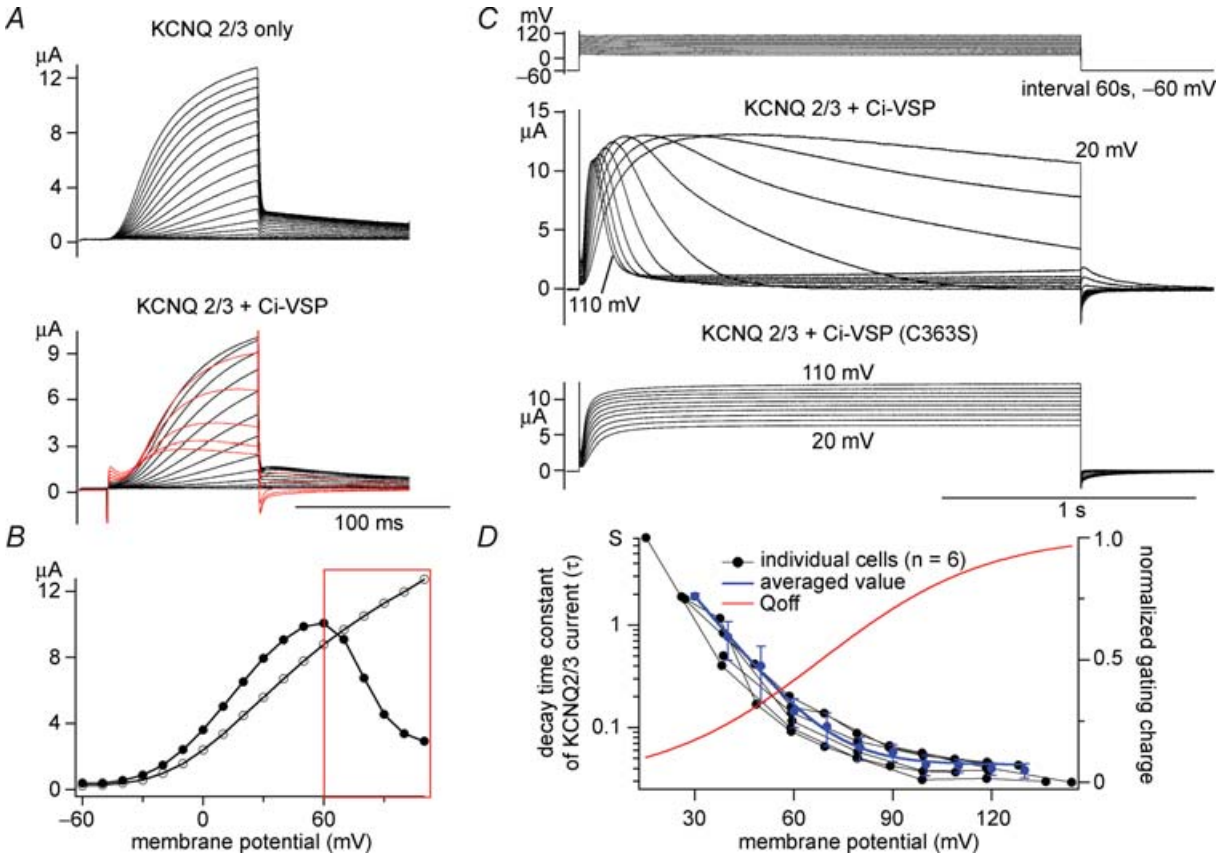

Figure 5. Decay of KCNQ2/3 current is induced by Ci-VSP in a voltage-dependent manner
A, KCNQ2/3 current coexpressed with (upper panel) or without (lower panel) Ci-VSP was recorded under the two-electrode voltage clamp. Holding potential was −60 mV, and step pulses were applied by 10 mV increment. KCNQ2/3 current showed 'inactivation-like' decay kinetics in the higher membrane potential condition (red traces). Transient outward notches at the onset of depolarization and inward notches at repolarization are 'gating' currents of Ci-VSP. Capacitative component was subtracted by *P*/–10 method. *B*, *I*–*V* relationships of traces shown in A (KCNQ2/3 only: open circles, KCNQ2/3 + Ci-VSP: filled circles) are shown. The red box indicates the voltage region where KCNQ2/3 current was decreased as shown in red traces in *A*. *C*, representative current traces with 'inactivation-like' decay kinetics of KCNQ2/3 currents (middle panel) by long depolarization (2 s). Intervals were set to 60 s at −60 mV (top panel). KCNQ2/3 coexpressed with enzyme-defective Ci-VSP mutant (C363S) did not exhibit such kinetics (bottom panel). Slowly activating outward current following decline of KCNQ2/3 current at high membrane potentials (ex. 110 mV) is probably due to endogenous current that often activates at this voltage range. *D*, voltage dependency of decay time constant of 'inactivation-like' kinetics in six oocytes. The decay phase of KCNQ2/3 current was fitted by single exponentials. The red curve is the charge–voltage curve (Q_{off}–V) adopted from our previous study (Murata *et al.* 2005).

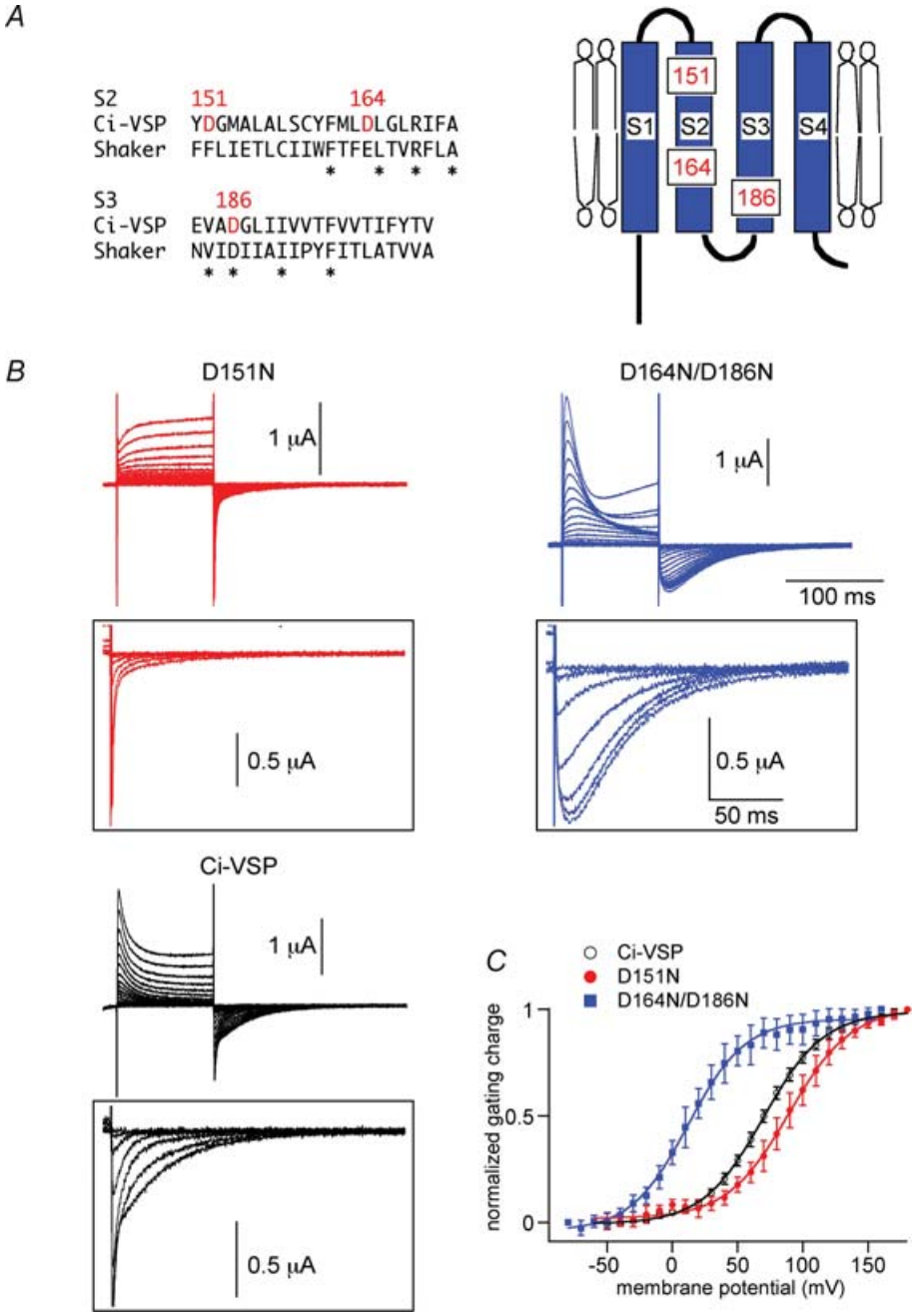

Figure 6. Shifted voltage dependency of 'gating' currents of the two VSD mutants, D164N/D186N and D151N

A, comparison of the amino acid sequence of S2 and S3 with *Shaker* potassium channel (left) and positions of negatively charged amino acid residues in the topology of the voltage sensor domain (right). *B*, representative traces of 'gating' current measurements under the two-electrode voltage clamp of D151N (red), wild-type (Ci-VSP), Ci-VSP (black) and D164N/D186N (blue). Holding potential was −60 mV and step pulses were applied from −60 mV to 180 mV for wild-type and D151N, from −80 mV to 160 mV for D164N/D186N by 10 mV increment. Symmetrical capacitive component was subtracted by the *P*/−10 method. OFF-'gating' current traces are indicated at higher magnification (lower panel). Traces are shown only from −60 mV to 120 mV for wild-type and D151N, −80 mV to 100 mV for D164N/D186N by 30 mV increment for clarity. *C*, Q_{off}–*V* curves of wild-type (black), D164N/D186N (blue) and D151N (red). The curve was fitted with the Boltzmann equation: $Q = Q_{max}/[1 + \exp\{zF(V_{1/2} - V)/RT\}]$. $V_{1/2}$ (mV) = 69.8 (Ci-VSP), 89.6 (D151N), 12.1 (D164N/D186N). z = 1.09 (wild-type), 1.06 (D151N), 1.15 (D164N/D186N).

negligible inward currents upon repolarization to −60 mV and the inward currents at repolarization from oocytes expressing Ci-VSP mainly reflect displacement currents. Uninjected oocytes showed only negligible fast-relaxing inward currents upon repolarization. Q_{off} under the TEVC provides an estimate of voltage dependency that is indistinguishable from that obtained by the measurements with the cut-open oocyte method, as previously demonstrated (Murata *et al.* 2005). When inward currents upon repolarization were integrated as 'Q_{off}' and plotted against the membrane potential, they showed a sigmoidal shape that is well fitted by a Boltzmann equation (Fig. 6*C*).

We exploited potential advantages of these mutants to test whether the shift of voltage dependency of phosphatase activities occurs correlated with the changes of voltage sensor movements. First, voltage-dependent decay of KCNQ2/3 outward current was compared among the two mutants and the wild-type (Fig. 7). With the step pulse to −20 mV or −10 mV for 4 s, D164N/D186N induced a clear decay of KCNQ2/3-derived outward current, whereas wild-type and D151N did not exhibit a current decay at this range of voltages (Fig. 7*A*). Plots of proportions of residual currents *versus* the peak amplitudes measured at distinct voltages indicate that D164N/D186N exhibits more significant decay than wild-type and D151N from −20 mV to 10 mV. At higher voltages, wild-type and D151N induced remarkable decay that becomes sharper as the voltage level increases. D151N exhibited less remarkable decay than the wild-type as seen from the plot of the residual component against the membrane potential (Fig. 7*B*). At more than 40 mV, the residual component is completely silenced in wild-type and D151N, whereas the decay kinetics of KCNQ2/3-derived current induced by D164N/D186N appears saturated and a significant residual current component was observed. This probably

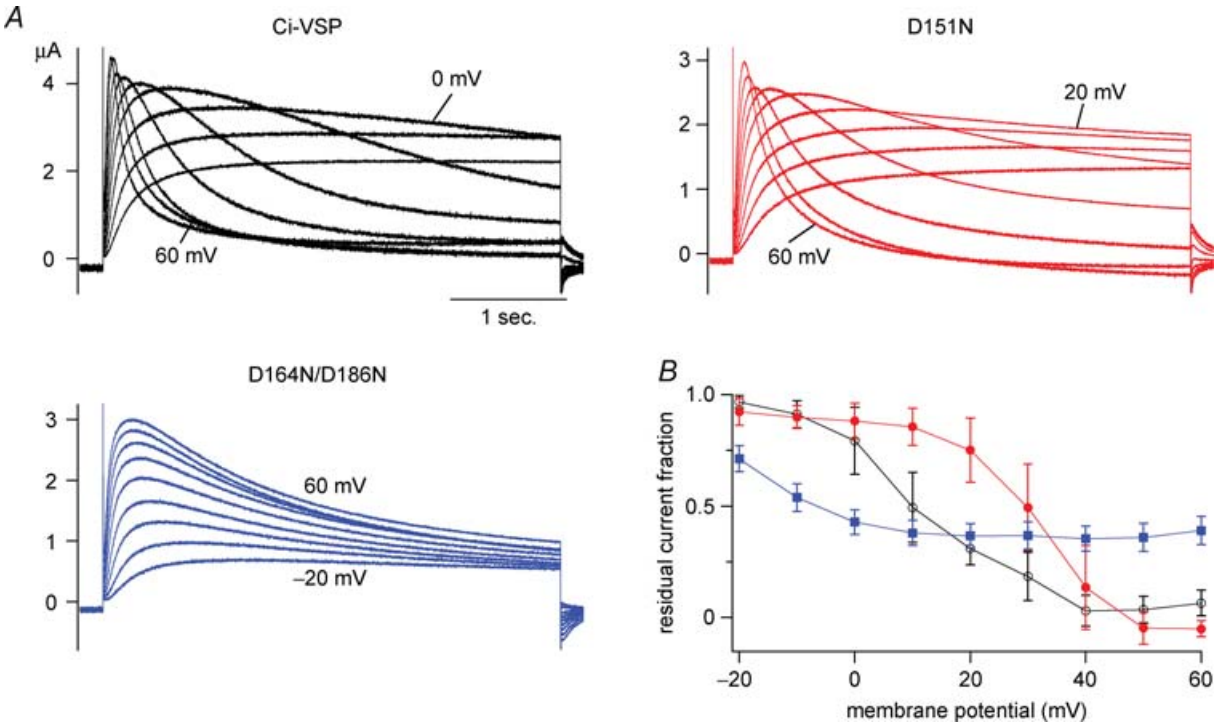

Figure 7. Induction of current decay of KCNQ2/3 channels occurs at lower membrane potential in D164N/D186N

A, representative traces of KCNQ2/3 potassium currents in the presence of Ci-VSP (black traces), D151N (red) or D164N/D186N (blue). Current traces were elicited by a depolarizing step to between −20 mV and 60 mV. At a higher voltage level, endogenous outward current was activated and superimposed. *B*, the magnitude of the residual component of KCNQ2/3 current during a 4 s step pulse was normalized by the peak amplitude at each membrane potential level. Data were recorded from a single batch of oocytes. The proportion of residual current was calculated for each trace as the ratio of the minimum current amplitude following the peak timing against the maximum amplitude. When there is no decay, the maximum magnitude during a 4 s step pulse was divided by the amplitude at the end of the pulse. Expression level of Ci-VSPs was estimated by the total moved charges, Q_{off}, of OFF-'gating' currents measured from another batch of oocytes that were microinjected with the same concentration of cRNA as for the measurement of KCNQ2/3 currents. Q_{off} values (nC) were -51.5 ± 12.2 (Ci-VSP), -39.6 ± 8.2 (D151N), -45.8 ± 11.4 (D164N/D186N), respectively. The numbers of cells were 5, 4, 4 for Ci-VSP, D151N and D164N/D186N, respectively. Similar results of the current decay of KCNQ2/3 channel were obtained from two other experiments.

suggests that D164N/D186N can attain only smaller maximum magnitude of phosphatase activity which is saturated at a lower voltage level than the wild-type and D151N. Plots of decay time constants of KCNQ2/3 current (Supplemental material Fig. S2) indicate that phosphatase activity D164N/D186N is only weakly voltage dependent at highly depolarized potentials. Despite an apparent decrease in maximal efficacy for phosphatase activity in D164N/D186N, the measurable voltage dependence for this mutant is clearly shifted toward more hyperpolarized potentials.

The voltage-dependent curve of Kir-reporting phosphatase activity is known to be slightly dependent on the expression level of Ci-VSP (Murata *et al.* 2005). The expression level of each version of Ci-VSP was therefore examined by measuring OFF-'gating' currents from sister oocytes (legend of Fig. 7) along with measurements of KCNQ2/3 currents. Although D151N exhibited slightly smaller magnitudes of 'gating' charges (39.6 ± 8.2 nC, $n = 9$), cells expressing D164N/D186N and wild-type expressed a similar magnitude of 'gating' charges (45.8 ± 11.4 nC, $n = 9$, 51.5 ± 12.2, $n = 10$, respectively).

Voltage dependency of phosphatase activity was also compared among the VSD mutants and the wild-type by measuring Kir currents. Holding the intervals to -40 mV led to only a small reduction of Kir amplitude in D151N, whereas more than 30% reduction was seen with D164N/D186N (Supplemental Fig. S1*A*). Plots of Kir activities against the holding potentials (Supplemental Fig. S1*C*) demonstrate a clear shift of voltage dependency of Kir-reporting phosphatase activities of D164/D184N from D151N. This shift of D164N/D186N was in the same direction as that of voltage dependency of the voltage-sensor movement. It is unlikely that the shifted voltage dependency of D164N/D184N is due to the different expression levels, since cells expressing D151N with different magnitudes of 'gating' charges showed significantly less negative values of $V_{1/2}$ than any set of data of D164N/D186N (Supplemental Fig. S1*D*).

These findings favour the idea that the VSD confers voltage dependency of the phosphatase.

Discussion

The high level of identity of amino acid sequence between the cytoplasmic region of Ci-VSP and PTEN and our previous findings (Murata *et al.* 2005) originally led us to propose that Ci-VSP exclusively dephosphorylates PtdIns(3,4,5)P_3 to increase the PtdIns(4,5)P_2 level. However, this idea clashes with several findings. (1) GIRK2 channel activities were drastically changed, given that GIRK2 may not discriminate between PtdIns(4,5)P_2 and PtdIns(3,4,5)P_3 (Fig. 3 in Rohacs *et al.* 1999). (2) GIRK2 and KCNQ2/3 channel activities are severely reduced or even abolished upon depolarization (Murata *et al.* 2005). (3) The range of membrane potentials which induced change of phosphatase activity as measured by GIRK2 channel activities was significantly shifted in a negative direction compared with the range of voltage sensor movement (Murata *et al.* 2005). In this study, the relationship between the carried charge of the VSD and phosphatase activity was studied through GFP-based confocal imaging and measurements of potassium channel activities. Our results indicate that phosphatase becomes active upon depolarization (Fig. 8), not upon hyperpolarization, unlike the originally proposed idea. Voltage-dependent properties of the current decay of KCNQ2/3 channel as well as run-down of the two types

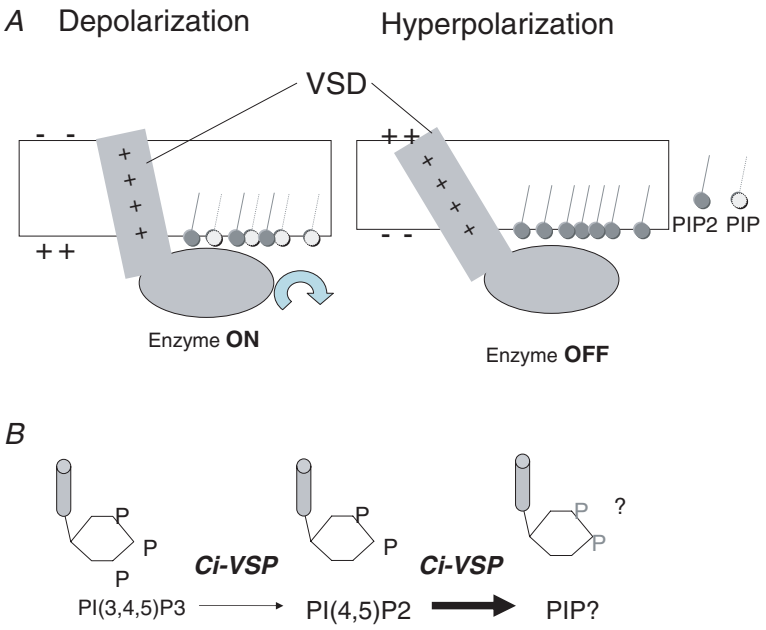

Figure 8. Scheme of operation of Ci-VSP
A, depolarization induces upward charge displacement of the voltage sensor and this triggers activation of phosphatase. *B*, Ci-VSP dephosphorylates not only PtdIns(3,4,5)P_3 but also PtdIns(4,5)P_2.

of Kir channels indicate that reduction of PtdIns(4,5)P_2 level by Ci-VSP can occur more significantly at higher membrane potentials. These observations are consistent with the ideas that not only PtdIns(3,4,5)P_3 but also PtdIns(4,5)P_2 is the substrate of phosphatase reaction by Ci-VSP and that these phosphatase activities are activated upon depolarization. We thus propose that Ci-VSP shares basic properties with voltage-gated Na^+, Ca^{2+}, and K^+ channels: (1) depolarization activates effector operation and (2) voltage-dependent conformational change of VSD is translated into a downstream effector.

Basic properties of Ci-VSP as phosphoinositide phosphatase

Our model predicts that phosphatase activity of Ci-VSP is silenced during hyperpolarization. This sounds paradoxical, given that phosphatase activity of *in vitro* purified cytoplasmic region of Ci-VSP (Murata *et al.* 2005) indicates that the VSD is not required for phosphatase activity. However, it is yet to be addressed whether *in vitro* measurements of phosphatase activities with purified recombinant protein consisting only of the cytoplasmic region represent enzyme activity in the resting state (corresponding to hyperpolarized condition) or activated state (corresponding to depolarized condition) of Ci-VSP. Furthermore, in an *in vitro* enzyme assay of recombinant cytoplasmic region, micelles but not native cell membranes were utilized. Under this condition, phosphoinositides could be randomly accessed to the active site of the phosphatase domain, whereas phosphoinostides are localized in the inner leaflet of the cell membrane in the environment of the *Xenopus* oocyte.

PTEN, which is highly homologous to the cytoplasmic region of Ci-VSP, has specificity for the 3-position of the inositol ring, and does not dephosphorylate PtdIns(4,5)P_2 (Maehama *et al.* 2001). Our conclusion is also inconsistent with previous findings that dephosphorylation by mammalian VSP orthologues is selective for the 3-position of inositol phosphates like PTEN (Walker *et al.* 2001; Wu *et al.* 2001). However, recent analysis of phosphatase specificity with a spectrum of fluorescence-labelled phosphoinositides by thin layer chromatography (H. Iwasaki, *et al.* in preparation, International Symposium of Kobe University, 2006), has indicated that PtdIns(4,5)P_2 is dephosphorylated *in vitro* by the cytoplasmic region of Ci-VSP.

Decrease of potassium channel activities induced by Ci-VSP

Understanding how fast phosphatase activity changes in Ci-VSP is an important issue in unravelling the mechanisms of coupling between VSD and the phosphatase domain. GIRK2 channels coexpressed with Ci-VSP decreased their current amplitude with a time constant of less than a second at 40 mV (Fig. 3). On coexpression with Ci-VSP, KCNQ2/3 channels showed voltage-dependent decay similar to N-type inactivation of voltage-gated potassium channels (Figs 5*C* and *D* and 7). This decay occurs with a time constant less than 50 ms at a level over 100 mV. These time scales of decay kinetics of potassium channels are much faster than the predicted turnover rate of the phosphatase activity of Ci-VSP, about several seconds per molecule, based on the *in vitro* measurements of enzyme kinetics of the recombinant phosphatase domain of Ci-VSP (Murata *et al.* 2005; Okamura, 2007). However, turnover rate by malachite green assay cannot simply be compared with kinetics of phosphatase activity in live cells due to the differences of conditions and configurations between the two measurements: (1) *in vitro* assays for measuring phosphatase activities utilize only the cytoplasmic region of the protein, which may only take a conformation corresponding to the resting state of the full-length protein under hyperpolarization in native membranes, as discussed before; (2) the alkyl chain of PtdIns(3,4,5)P_3 utilized for that assay is shorter than native phosphoinositides; (3) micelles containing phosphoinisitides, not the native cell membrane, were used in the *in vitro* assay; and (4) PtdIns(4,5)P_2 was not used, but PtdIns(3,4,5)P_3 was utilized for the *in vitro* assay (Murata *et al.* 2005), whereas PtdIns(4,5)P_2 is likely to be a more abundant substrate *in vivo*. It is also possible that the potassium channel could be spatially colocalized with Ci-VSP and depletion of PtdIns(4,5)P_2 just close to potassium channels occurs much faster than the global PtdIns(4,5)P_2 in the cell membrane.

The decay kinetics of potasium channels may also depend on many other factors than enzyme kinetics. These factors may include local diffusion of PtdIns(4,5)P_2, unbinding of PtdIns(4,5)P_2 from the potassium channel, and a delay in the closing of the potassium channel after the unbinding of PtdIns(4,5)P_2. In addition, kinetics of current decay also depend on sensitivity of channel activities to phosphoinositides and the robustness of expression of Ci-VSP. In fact, the time course of GIRK2 channel activities with depolarizing intervals (Fig. 3*B* and *C*) was significantly faster than the decay kinetics of KCNQ2/3 channel-derived outward currents (Fig. 5*C* and *D*) when compared at the same membrane potentials. Such a difference in time course can be expected given that the GIRK2 channel requires a higher concentration of PtdIns(4,5)P_2 for activity than KCNQ2/3 channels.

More studies will be required to clarify how decay of potassium channel activity is quantitatively correlated with the kinetics of the phosphatase. It is unlikely that voltage-dependent decay of KCNQ2/3 channel currents in the presence of Ci-VSP is derived from the intrinsic voltage

sensor of KCNQ2/3 channels, or any voltage-dependent mechanism that is unrelated to the activity of Ci-VSP. In Kv1 potassium channels, PtdIns(4,5)P_2 is known to modulate N-type inactivation by binding to an inactivation ball region (Oliver *et al.* 2004). However, the KCNQ2/3 channel does not have any cytoplasmic structure of the inactivation ball and does not interact with the potassium channel β-subunit that operates as the inactivation ball. Voltage-dependent decay of the KCNQ2/3 channel is not observed under PtdIns(4,5)P_2 depletion, which is induced by activation of phospholipase C (Nakajo & Kubo, 2005).

Coupling between VSD and the phosphatase domain

The voltage-dependent change of phosphatase activity reported by GIRK2 channel activity was saturated at depolarization, around +20 mV, at which only about 10–15% of the total charge of the voltage sensor moves (Murata *et al.* 2005). This apparent gap of voltage dependency between the charge movement and phosphatase activity was due to the limited dynamic range of sensitivity of GIRK2 channels to phosphoinositides. In fact, measurements of GIRK2 activities coexpressed with Ci-VSP in the present study indicate that changes in concentration of PtdIns(4,5)P_2 occur in a time scale of less than 0.5 s upon depolarization to 0 mV and this kinetics becomes gradually sharper from 0 mV to 40 mV. Voltage-dependent change of IRK1-reporting PtdIns(4,5)P_2 concentration indicates that phosphatase activity of Ci-VSP is enhanced up to 50 mV (Fig. 4). KCNQ2/3 channels coexpressed with Ci-VSP exhibited voltage-dependent current decay that became sharper over a range of membrane potentials up to 100 mV. These results suggest that enzyme activity in Ci-VSP is gradually changed over a range of membrane potentials where the magnitude of 'gating' charges of the VSD varies.

The mild steepness and wide range of voltage dependency of phosphatase activity in Ci-VSP contrast with voltage-gated ion channels in which allosteric interaction among four homologous domains enables a sharp voltage-dependent increase in the probability of pore opening at no more than 10 mV. The Q–V curve of 'gating' currents of Ci-VSP is less steep than that of voltage-gated potassium channels, but this probably cannot fully account for milder voltage dependency of phosphatase activity than that of voltage-dependent gating of ion channels. Recent X-ray crystallography of the mammalian Kv1.2 channel indicated that four subunits interact with each other, and VSD is in close proximity to the pore domain of the neighbouring subunit (Long *et al.* 2005). Synergetic interactions between the four VSDs through pore regions enable sharp voltage-dependent activation of voltage-gated ion channels. Possibly, VSP may operate in a simpler way: the voltage sensor movement is translated into activation of phosphatase activity without requiring protein–protein or intersubunit interactions. This must require further characterization of the quantitative correlation between the VSD movement and phosphatase activity as well as the elucidation of the subunit stoichiometry. In this context, a version with mutations in the VSD, D164N/D186N, will serve as a good model to understand mechanisms of coupling between the VSD and phosphatase, since it exhibited both slowed 'gating' currents and reduced phosphatase activity as seen from the slow decay kinetics of KCNQ2/3 channels (Fig. 7*A*). It will be important to determine how the maximum scale of enzyme activity is blunted or kinetics of activation of enzyme activity is modified in this mutant.

Why has nature developed the property of Ci-VSP that phosphatase activity is tuned at a level of membrane potential over 0 mV, which cannot be physiologically attained in many types of cells? In mammalian phagocytes, large depolarizations of more than 40 mV can take place due to oxidase activity (Banfi *et al.* 1999). Intriguingly, Ci-VSP is expressed in blood cells of ascidians, *Ciona intestinalis* (personal communcation from Dr M. Ogasawara). Ci-VSP may play a role in translating an electrical signal into a chemical signal, not within a narrow window of membrane potential such as for generation of action potentials in neurons and muscle, but rather over a wide range of membrane potentials that probably may be attained physiologically in these cells.

References

Banfi B, Schrenzel J, Nusse O, Lew DP, Ligeti E, Krause KH & Demaurex N (1999). A novel H^+ conductance in eosinophils: unique characteristics and absence in chronic granulomatous disease. *J Exp Med* **190**, 183–194.

Bezanilla F (2000). The voltage sensor in voltage-dependent ion channels. *Physiol Rev* **80**, 555–592.

DeCoursey TE, Cherny VV, Zhou W & Thomas LL (2000). Simultaneous activation of NADPH oxidase-related proton and electron currents in human neutrophils. *Proc Natl Acad Sci U S A* **97**, 6885–6889.

Demaurex N, Grinstein S, Jaconi M, Schlegel W, Lew DP & Krause KH (1993). Proton currents in human granulocytes: regulation by membrane potential and intracellular pH. *J Physiol* **466**, 329–344.

Fukuda M, Kojima T, Kabayama H & Mikoshiba K (1996). Mutation of the pleckstrin homology domain of Bruton's tyrosine kinase in immunodeficiency impaired inositol 1,3,4,5-tetrakisphosphate binding capacity. *J Biol Chem* **271**, 30303–30306.

Goldin AL (1992). Maintenance of *Xenopus laevis* and oocyte injection. *Methods Enzymol* **207**, 266–279.

Hille B (2001). *Ion Channels of Excitable Membranes*. Sinauer, Sunderland, MA, USA.

Huang CL, Feng S & Hilgemann DW (1998). Direct activation of inward rectifier potassium channels by PIP_2 and its stabilization by $G\beta\gamma$. *Nature* **391**, 803–806.

Jaffe LA (1976). Fast block to polyspermy in sea urchin eggs is electrically mediated. *Nature* **261**, 68–71.

Levin M, Thorlin T, Robinson KR, Nogi T & Mercola M (2002). Asymmetries in H^+/K^+-ATPase and cell membrane potentials comprise a very early step in left-right patterning. *Cell* **111**, 77–89.

Long SB, Campbell EB & MacKinnon R (2005). Crystal structure of a mammalian voltage-dependent Shaker family K^+ channel. *Science* **309**, 897–903.

Lu Z, Klem AM & Ramu Y (2001). Ion conduction pore is conserved among potassium channels. *Nature* **413**, 809–813.

Maehama T & Dixon JE (1998). The tumor suppressor, PTEN/MMAC1, dephosphorylates the lipid second messenger, phosphatidylinositol 3,4,5-trisphosphate. *J Biol Chem* **273**, 13375–13378.

Maehama T, Taylor GS & Dixon JE (2001). PTEN and myotubularin: novel phosphoinositide phosphatases. *Annu Rev Biochem* **70**, 247–279.

Murata Y (2006). Voltage sensor domain drives modification of phosphatase activity of the voltage-sensor containing phosphatase, Ci-VSP. *Biophys J*, 2006 Abstracts Issue, 2656-Pos.

Murata Y, Iwasaki H, Sasaki M, Inaba K & Okamura Y (2005). Phosphoinositide phosphatase activity coupled to an intrinsic voltage sensor. *Nature* **435**, 1239–1243.

Nakajo K & Kubo Y (2005). Protein kinase C shifts the voltage dependence of KCNQ/M channels expressed in *Xenopus* oocytes. *J Physiol* **569**, 59–74.

Okamura Y (2007). Biodiversity of voltage-sensor domain proteins. *Pflugers Arch* **454**, 361–371.

Oliver D, Lien CC, Soom M, Baukrowitz T, Jonas P & Fakler B (2004). Functional conversion between A-type and delayed rectifier K^+ channels by membrane lipids. *Science* **304**, 265–270.

Ramsey IS, Moran MM, Chong JA & Clapham DE (2006). A voltage-gated proton-selective channel lacking the pore domain. *Nature* **440**, 1213–1216.

Rohacs TCJ, Prestwich GD & Logothetis DE (1999). Distinct specificities of inwardly rectifying K^+ channels for phosphoinositides. *J Biol Chem* **274**, 36065–36072.

Salim K, Bottomley MJ, Querfurth E, Zvelebil MJ, Gout I, Scaife R, Margolis RL, Gigg R, Smith CI, Driscoll PC, Waterfield MD & Panayotou G (1996). Distinct specificity in the recognition of phosphoinositides by the pleckstrin homology domains of dynamin and Bruton's tyrosine kinase. *EMBO J* **15**, 6241–6250.

Sasaki M, Takagi M & Okamura Y (2006). A voltage sensor-domain protein is a voltage-gated proton channel. *Science* **312**, 589–592.

Stauffer TP, Ahn S & Meyer T (1998). Receptor-induced transient reduction in plasma membrane PtdIns(4,5)P_2 concentration monitored in living cells. *Curr Biol* **8**, 363–366.

Tombola F, Pathak MM & Isacoff EY (2006). How does voltage open an ion channel? *Annu Rev Cell Dev Biol* **22**, 23–52.

Varnai P & Balla T (1998). Visualization of phosphoinositides that bind pleckstrin homology domains: calcium- and agonist-induced dynamic changes and relationship to myo-[^{3}H]inositol-labeled phosphoinositide pools. *J Cell Biol* **143**, 501–510.

Varnai P, Rother KI & Balla T (1999). Phosphatidylinositol 3-kinase-dependent membrane association of the Bruton's tyrosine kinase pleckstrin homology domain visualized in single living cells. *J Biol Chem* **274**, 10983–10989.

Walker SM, Downes CP & Leslie NR (2001). TPIP: a novel phosphoinositide 3-phosphatase. *Biochem J* **360**, 277–283.

Wang HS, Pan Z, Shi W, Brown BS, Wymore RS, Cohen IS, Dixon JE & McKinnon D (1998). KCNQ2 and KCNQ3 potassium channel subunits: molecular correlates of the M-channel. *Science* **282**, 1890–1893.

Wu Y, Dowbenko D, Pisabarro MT, Dillard-Telm L, Koeppen H & Lasky LA (2001). PTEN 2, a Golgi-associated testis-specific homologue of the PTEN tumor suppressor lipid phosphatase. *J Biol Chem* **276**, 21745–21753.

Zhang H, Craciun LC, Mirshahi T, Rohacs T, Lopes CM, Jin T & Logothetis DE (2003). PIP_2 activates KCNQ channels, and its hydrolysis underlies receptor-mediated inhibition of M currents. *Neuron* **37**, 963–975.

Zhang L, Lee JK, John SA, Uozumi N & Kodama I (2004). Mechanosensitivity of GIRK channels is mediated by protein kinase C-dependent channel-phosphatidyl inositol 4,5-bisphosphate interaction. *J Biol Chem* **279**, 7037–7047.

Zhang C & Zhou Z (2002). Ca^{2+}-independent but voltage-dependent secretion in mammalian dorsal root ganglion neurons. *Nat Neurosci* **5**, 425–430.

Acknowledgements

We thank anonymous referees for helpful comments and improving our manuscript. We thank Drs M. Takano (Jichii Medical University), N. Uozumi and J. K. Lee (Tohoku University) for providing PH_{PLC}–GFP plasmid, Dr M. Fukuda (Tohoku University) for PH_{Btk}–GFP plasmid, Dr H. Iwasaki for sharing his preliminary results and ideas of phosphatase substrate specificity and helpful discussion throughout this study, and Drs Laurinda Jaffe and T. McCormack for both scientific and editorial comments on the manuscript. This work is supported by Research Fellowships of the Japan Society for the Promotion of Science for Young Scientists to Y.M. and a Grant-in-Aid for Scientific Research from Ministry of Education, Culture, Sports, Science and Technology to Y.O.

Supplemental material

Online supplemental material for this paper can be accessed at:
http://jp.physoc.org/cgi/content/full/jphysiol.2007.134775/DC1
and
http://www.blackwell-synergy.com/doi/suppl/10.1113/jphysiol.2007.134775